Cubical Cohomology Ring of 3D Photographs

Rocio Gonzalez-Diaz, Maria Jose Jimenez, Belen Medrano
Applied Math Department (I), School of Computer Engineering, University of Seville, Spain

Received 3 February 2010; accepted 8 October 2010

ABSTRACT: Cohomology groups and the cohomology ring of three-dimensional (3D) objects are topological invariants that characterize holes and their relations. Cohomology ring has been traditionally computed on simplicial complexes. Nevertheless, cubical complexes deal directly with the voxels in 3D images, no additional triangulation is necessary. This could facilitate efficient algorithms for the computation of topological invariants in the image context. In this article, we present a constructive process, made up by several algorithms, to compute the cohomology ring of 3D binary-valued digital photographs represented by cubical complexes. Starting from a cubical complex Q that represents such a 3D picture whose foreground has one connected component, we first compute the homological information on the boundary of the object, ∂Q, by an incremental technique; using a face reduction algorithm, we then compute it on the whole object; finally, applying explicit formulas for cubical complexes (without making use of any additional triangulation), the cohomology ring is computed from such information. Int J Imaging Syst Technol, 21, 76–85, 2011; Published online in Wiley Online Library (wileyonlinelibrary.com). DOI 10.1002/ima.20271

Key words: cohomology ring; cubical complexes; 3D digital images

1. INTRODUCTION

Many computer application areas involve topological methods which usually mean a significant reduction in the amount of data. Homology groups are algorithmically computable topological invariants that characterize an object by its ''holes'' (in any dimension). Informally, the connected components of a three dimentional (3D)-object are the holes in dimension (dim.) 0, the tunnels are the holes in dim. 1 and the cavities the ones in dim. 2. Cohomology groups are topological invariants that represent an algebraic duality of homology groups. Although the formal definition of cohomology groups is motivated primarily by algebraic considerations, homology and cohomology groups of 3D objects are isomorphic, that is, they provide the same topological information. Nevertheless, cohomology groups have an additional ring structure provided by the cup product (denoted by $\smile$). The cup product can be seen as the way the holes obtained in homology are related to each other. For example, think of the torus, and the wedge sum of two loops and a 2-sphere (see Fig. 1). Both objects have two tunnels and one cavity; but the cavity (γ) of the first object can be decomposed in the product of the two tunnels (α and β), that is, $\alpha\smile\beta = \gamma$, whereas the cavity of the second object cannot. This information contributes to a better understanding of the degree of topological complexity of the analyzed digital object, and sheds light on its geometric features.

In (Gonzalez-Diaz and Real, 2003, 2005), a method for computing the cohomology ring of 3D binary digital images is described. In those papers, the cohomology ring computation is performed over a simplicial complex K associated with the digital binary-valued picture using the 14-adjacency, applying the known formulas for computing the cohomology ring of any simplicial complex (see Munkres, 1984). In (Molina-Abril and Real, 2008), a particular cell structure provided by the 26-adjacency is associated with a given 3D picture for computing homology groups. However, one could assert that a more natural combinatorial structure when dealing with 3D digital images is the one provided by cubical complexes. In (Gonzalez-Diaz et al., 2009b), we presented formulas to directly compute the cohomology ring of 3D cubical complexes without making use of additional triangulations. In this article, given a 3D digital image I, we consider the cubical complex Q whose elements are the unit cubes (voxels) of the foreground of I together with all their faces. We describe a strategy to tackle the cohomology ring computation on a 3D binary-valued digital picture: we first compute the homology of the ''boundary'' of Q, denoted by ∂Q; second, using a face reduction technique, we obtain a cell complex K with the same topological information than Q but with far fewer cells, which makes possible the reduction of the complexity of the computation of the cup product. Finally, we compute the cohomology ring of K and give a procedure to translate the results obtained to the digital image I.

This article is organized as follows. In Section 2, we recall the concept of AT-model (Gonzalez-Diaz and Real, 2003, 2005) for a polyhedral cell complex P, which consists of an algebraic set of data that provides homological information of P. Given an AT-model for a polyhedral cell complex, we provide the formulas of a new AT-model obtained after a subdivision; this result is the key to prove the validity of the formulas for computing the cohomology ring of 3D cubical complexes established in Section 3. Section 4 is devoted to describe a process to obtain an AT-model of a given 3D digital image I that provides the ingredients for computing the cohomology ring of I. Finally, some conclusions and plans for future are drawn in Section 5.

A preliminary version of this article was presented at the 13th International Workshop on Combinatorial Image Analysis.

Correspondence to: Rocio Gonzalez-Diaz; e-mail: rogodi@us.es

Grant sponsor: Junta de Andalucia Research Group FQM-296

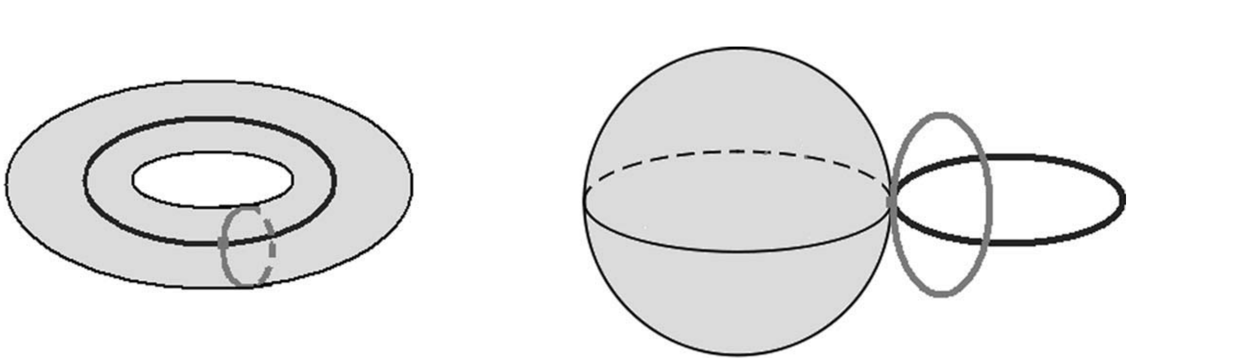

Figure 1. On the left, a hollow torus and its two tunnels. On the right, the wedge sum of a 2-sphere and two loops.

2. AT -MODELS FOR POLYHEDRAL CELL COMPLEXES

Since we are working with objects embedded in $\mathbb{R}^3$, homology groups are torsion-free (Alexandroff and Hopf, 1935. ch. 10), so computing homology over a field is enough to characterize shapes (Munkres, 1984; p 332). This fact, together with the isomorphism (over any field) between homology and cohomology groups (Munkres, 1984; p. 320), enables us to consider $Z/2$ as the ground ring throughout this article.

Definition 1. A polyhedral cell complex P in $\mathbb{R}^3$, is given by a finite collection of cells, which are convex polytopes (vertices, edges, polygons, and polyhedra), together with all their faces and such that the intersection between any two of them is either empty or a face of each of them. A proper face of $\sigma \in P$ is a face of σ whose dimension is strictly less than the one of σ. A facet of σ is a proper face of σ of maximal dimension. A maximal cell of P is a cell of P, which is not a proper face of any other cell of P.

Observe that if the cells of P are n—simplices, P is a simplicial complex (Munkres, 1984); in the case that the cells of P are n—cubes, then P is a cubical complex (see for example (Kaczynski et al., 2004)). A q-cell of either a simplicial complex or a cubical complex can be denoted by the list of its vertices.

For any graded set $S = \{S_q\}_q$, one can consider formal sums of elements of S_q, which are called q—chains, and which form abelian groups with respect to the component-wise addition (module (mod) 2). These groups are called q—chain group denoted by C_q (S). The collection of all the chain groups associated with S is denoted by C (S), that is $C(S) = \{C_q(S)\}_q$, and also called chain group, for simplicity. Let $\{s_1, \ldots, s_m\}$ be the elements of S_q for a fixed q. Given two q-chains $c_1 = \sum_{i=1}^m \lambda_i s_i$ and $c_2 = \sum_{i=1}^m \mu_i s_i$, where $\lambda_i, \mu_i \in Z/2$ for $i = 1, \ldots, m$, the expression $\langle c_1, c_2 \rangle$ refers to $\sum_{i=1}^m \lambda_i \cdot \mu_i \in Z/2$. For example, fixed i and j, the expression $\langle c_1, s_i \rangle$ is λ_i and $\langle s_i, s_j \rangle$ is 1 if $i = j$ and 0 otherwise.

Definition 2. The polyhedral chain complex associated with the polyhedral cell complex P is the collection $C(P) = \{C_q(P), \partial_q\}_q$ where:

- Each C_q (P) is the corresponding chain group generated by the q-cells of P;
- The boundary operator $\partial_q : C_q(P) \to C_{q-1}(P)$ connects two immediate dimensions.

The boundary of a q-cell is the formal sum of all its facets. It is extended to q-chains by linearity.

For example, consider a triangle (v_i, v_j, v_k) with vertices v_i, v_j, v_k. The boundary of the triangle is the formal sum of its edges, that is, $\partial_2\,(v_i, v_j, v_k) = (v_i, v_j) + (v_j, v_k) + (v_i, v_k)$.

Definition 3. Given a polyhedral cell complex P, an algebraic-topological model (AT-model (Gonzalez-Diaz and Real, 2003, 2005)) for P is a set of data (P, H, f, g, ϕ), where H is a graded subset of P and f, g, and ϕ are three families of maps $\{f_q : C_q(P) \to C_q(H)\}_q$, $\{g_q : C_q(H) \to C_q(P)\}_q$, and $\{\phi_q : C_q(P) \to C_{q+1}(P)\}_q$, such that, for each q:

1. $f_q g_q = \mathrm{id}_{C_q(H)}$, $\phi_{q-1}\partial_q + \partial_{q+1}\phi_q = \mathrm{id}_{C_q(P)} + g_q f_q$;
2. $f_{q-1}\partial_q = 0$, $\partial_q g_q = 0$;
3. $\phi_{q+1}\phi_q = 0, f_{q+1}\phi_q = 0$, $\phi_q g_q = 0$;

where $\mathrm{id}_{C_q(H)}$ and $\mathrm{id}_{C_q(P)}$ are the identity maps.

As a result, the chain group C (H) is isomorphic to the homology (and to the cohomology) of P. In particular, the number of vertices of H coincides with the number of connected components of P, the number of edges of H with the number of tunnels of P and the number of 2-cells of H with the number of cavities of P. Fixed q, for each $\sigma \in H_q$, $g_q(\sigma)$ is a representative cycle of a homology generator of dim. q.

Define an homomorphism $\sigma^* f_q : C_q(P) \to Z/2$ such that if μ is a q-cell of P,

$$\sigma^* f_q(\mu) := \langle \sigma, f_q(\mu) \rangle \ \ mod\ 2.$$

Then, $\sigma^* f_q$ is a representative cocycle of a cohomology generator of dim. q. An isomorphism between C (H) and the homology (respectively (resp.) cohomology) of P maps each $\sigma \in H$ to the homology class represented by $g_q(\sigma)$ (resp. the cohomology class represented by $\sigma^* f_q$) (see (Gonzalez-Diaz and Real, 2003, 2005)).

From now on, we will omit subscripts for simplicity.

Example 1. Let Q be an abstract cubical representation of the hollow torus (see Fig. 2). An AT-model for Q is the set of data (Q, H, f, g, ϕ) given in Table I, where $a_1 \in \{(v_3, v_6), (v_4, v_8)\}$; $a_2 \in \{(v_1, v_7), (v_2, v_8)\}$; $b_1 = (v_0, v_2)$; $b_2 = (v_0, v_4)$; $c = (v_0, v_2, v_4, v_8)$; $\gamma_{(v_i}, v_0)$ is the only path in Q from v_i to v_0 given in Figure 2 (on the center). For example, $\gamma_{(v_7}, v_0) = (v_5, v_7) + (v_1, v_5) + (v_0, v_1)$. Given an edge e of Q, c_e is the sum of the squares that correspond to the ''path'' starting from e and following the arrows in Figure 2 (on the right). For example, $c_{(v_1}, v_7) = (v_0, v_1, v_4, v_7) + (v_3, v_5, v_4, v_7) + (v_0, v_1, v_3, v_5)$. Representative cycles of homology generators are the vertex v_0, the tunnels $\alpha_1 = (v_0, v_1) + (v_1, v_2) + (v_0, v_2)$ and α $(v_0, v_3) + (v_3, v_4) + (v_0, v_4)$ and the cavity β which is the sum of the nine squares of Q.

An algorithm for computing AT-models for polyhedral cell complexes appears for example in (Gonzalez-Diaz and Real, 2003, 2005). In fact, in those papers, the algorithm is designed for simplicial complexes but the adaptation to polyhedral cell complexes is straightforward. That algorithm runs in time $O(m^3)$ where m is the

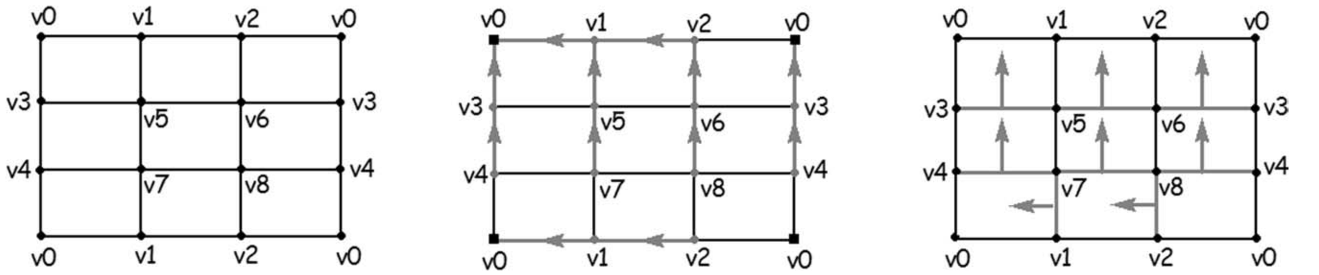

Figure 2. On the left, an abstract cubical representation Q of the hollow torus. On the center, the path $Y(v_i, v_0)$, for each vertex v_i of Q. On the right, the "path" c_e, for each edge e of Q.

number of cells of the given polyhedral cell complex. If an AT-model (P, H, f, g, ϕ) for a polyhedral cell complex P is computed using that algorithm then it is also satisfied that if $a \in H$ then $f(a) = a$ and $a \in g(a)$.

Let P be a polyhedral cell complex. Fixed q, we say that a q-cell $\alpha \in P$ is subdivided into two new q-cells $\alpha_1 \notin P$ and $\alpha_2 \notin P$ by a new $(q-1)$-cell $e \notin P$ (see, for example, Fig. 3) if:

- e is a facet of α_1 and α_1;
- $\alpha_1 \cup \alpha_1 = \alpha$;
- $\alpha_1 \cap \alpha_1 = e$.

The following lemma establishes how to obtain a new AT-model for P after subdividing a q-cell α of P by a $(q-1)$-cell e into two new q-cells α_1 and α_1. This result is used to prove the equivalence between the formula to directly compute the cup product on cubical complexes and the classical one on simplicial complexes.

Lemma 1. Let (P, H, f, g, ϕ) be an AT-model for a polyhedral cell complex P computed using the algorithm given in (Gonzalez-Diaz and Real, 2003, 2005). Let α be a q-cell, which is subdivided into two new q-cells α_1 and α_1 by a new $(q-1)$-cell e. Let $H' := (H\backslash\{\alpha\}) \cup \{\alpha_1\}$ if $\alpha \in H$, and $H' := H$ otherwise; $P' := (P\backslash\{\alpha\}) \cup \{\alpha_1, \alpha_1, e\}$; and ∂' the boundary operator of P' given by: $\partial'(c) := \partial(c) + \langle \alpha, \partial(c)\rangle(\alpha + \alpha_1 + \alpha_1)$ for any $c \in P'\backslash\{e, \alpha_1, \alpha_1\}$. Denote $\partial(\alpha_1) + e$ by A, and $\partial(\alpha_1) + e$ by B. Then, the set (P', H', f', g', ϕ') is an AT-model for P', where f', g', and ϕ' are given by:

- $f'(\alpha_1) := f(\alpha) + \langle\alpha, f(\alpha)\rangle(\alpha+\alpha_1)$; $f'(\alpha_2) := 0$;
  $f'(e) := f(A) = f(B)$;
  $f'(\sigma) := f(\sigma) + \langle\alpha, f(\sigma)\rangle(\alpha+\alpha_1)$, for any $\sigma \in P'\backslash\{\alpha_1, \alpha_2, e\}$;
- $\phi'(\alpha_1) := \phi(\alpha)$; $\phi'(\alpha_2) := 0$; $\phi'(e) := \alpha_2 + \phi(B) + \langle\alpha, \phi(B)\rangle(\alpha+\alpha_1+\alpha_2)$;
  $\phi'(\sigma) := \phi(\sigma) + \langle\alpha, \phi(\sigma)\rangle(\alpha+\alpha_1+\alpha_2)$ $\sigma \in P'\backslash\{\alpha_1, \alpha_2, e\}$
- If αH, $g'(\alpha_1) := g(\alpha) + \alpha + \alpha_1 + \alpha_2$;
  $g'(\gamma) := g(\gamma) + \langle\alpha, g(\gamma)\rangle(\alpha+\alpha_1+\alpha_2)$, for any $\gamma \in H'\backslash\{\alpha_1\}$

Table I. An AT-model for the abstract cubical representation of the hollow torus Q given in Figure 2

Q	f	ϕ	H	g
v_0	v_0	0	v_0	v_0
$v_i, i = 1,\ldots, 8$	v_0	$\gamma(v_i, v_0)$		
a_i, $i = 1,2$	b_i	c_{a_i}		
b_i, $i = 1,2$	b_i	0	b_i	α_i
Any edge $b \neq a_i, b_i$	0	c_b		
c	c	0	c	β
Any square $\sigma \neq c$	0	0		

Proof. We have to check that (P', H', f', g', ϕ') is an AT-model for P'. We will only check that $f'g' = \text{id}$ and $\text{id} + g'f' = \phi'\partial' + \partial'\phi'$. The rest of the conditions are left to the reader. Let $\gamma \in H'$, $\gamma \neq \alpha_1$, and $\sigma \in P'\backslash\{\alpha$.

1. $f'g' = \text{id}$:

$$\begin{aligned} f'g'(\gamma) &= f'(g(\gamma) + \langle\alpha, g(\gamma)\rangle\alpha) + \langle\alpha, g(\gamma)\rangle f'(\alpha_1) \\ &= fg(\gamma) + \langle\alpha, g(\gamma)\rangle f(\alpha) \\ &\quad + \langle\alpha, g(\gamma)\rangle\langle\alpha, f(\alpha)\rangle(\alpha+\alpha_1) + \langle\alpha, g(\gamma)\rangle(f(\alpha) \\ &\quad + \langle\alpha, f(\alpha)\rangle(\alpha+\alpha_1)) = \gamma. \end{aligned}$$

If $\alpha \in H$: $f'g'(\alpha_1) = f'(g(\alpha)+\alpha) + f'(\alpha_1)$
$= f(g(\alpha)+\alpha) + f(\alpha) + \alpha + \alpha_1 = \alpha_1$.

2. $\text{id} + g'f' = \phi'\partial' + \partial'\phi'$:

$$\begin{aligned} \alpha_1 + g'f'(\alpha_1) &= \alpha_1 + g'(f(\alpha) + \langle\alpha, f(\alpha)\rangle\alpha) + \langle\alpha, f(\alpha)\rangle g'(\alpha_1) \\ &= \alpha_1 + g(f(\alpha) + \langle\alpha, f(\alpha)\rangle\alpha) + \langle\alpha, g(f(\alpha) \\ &\quad + \langle\alpha, f(\alpha)\rangle\alpha)\rangle(\alpha+\alpha_1+\alpha_2) + \langle\alpha, f(\alpha)\rangle g(\alpha) \\ &\quad + \langle\alpha, f(\alpha)\rangle(\alpha+\alpha_1+\alpha_2) \\ &= \alpha_1 + gf(\alpha) + \langle\alpha, gf(\alpha) + \langle\alpha, f(\alpha)\rangle g(\alpha)\rangle(\alpha+\alpha_1+\alpha_2) \\ &\quad + \langle\alpha, f(\alpha)\rangle(\alpha+\alpha_1+\alpha_2) + \langle\alpha, f(\alpha)\rangle(\alpha+\alpha_1+\alpha_2) \\ &= \alpha_1 + gf(\alpha) + \langle\alpha, gf(\alpha)\rangle(\alpha+\alpha_1+\alpha_2) \\ &= \alpha_1 + \alpha + \phi(A) + \phi(B) + \partial\phi(\alpha) + \alpha + \alpha_1 + \alpha_2 \\ &\quad + \langle\alpha, \phi\partial(\alpha)\rangle(\alpha+\alpha_1+\alpha_2) + \langle\alpha, \partial\phi(\alpha)\rangle(\alpha+\alpha_1+\alpha_2) \\ &= \alpha_2 + \phi(B) + \langle\alpha, \phi(B)\rangle(\alpha+\alpha_1+\alpha_2) + \phi(A) \\ &\quad + \langle\alpha, \phi(A)\rangle(\alpha+\alpha_1+\alpha_2) + \partial\phi(\alpha) + \langle\alpha, \partial\phi(\alpha)\rangle(\alpha+\alpha_1+\alpha_2) \\ &= \phi'\partial'(\alpha_1) + \partial'\phi'(\alpha_1). \end{aligned}$$

$$\begin{aligned} \phi'\partial'(\alpha_2) + \partial'\phi'(\alpha_2) &= \phi'(e) + \phi'(B) \\ &= \alpha_2 + \phi(B) + \langle\alpha, \phi(B)\rangle(\alpha+\alpha_1+\alpha_2) + \phi(B) \\ &\quad + \langle\alpha, \phi(B)\rangle(\alpha+\alpha_1+\alpha_2) \\ &= \alpha_2 = \alpha_2 + g'f'(\alpha_2). \end{aligned}$$

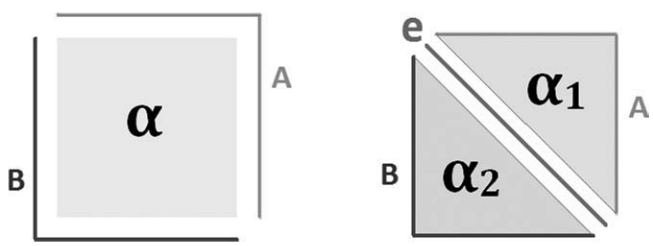

Figure 3. A subdivision of a square α in two triangles α_1 and α_2.

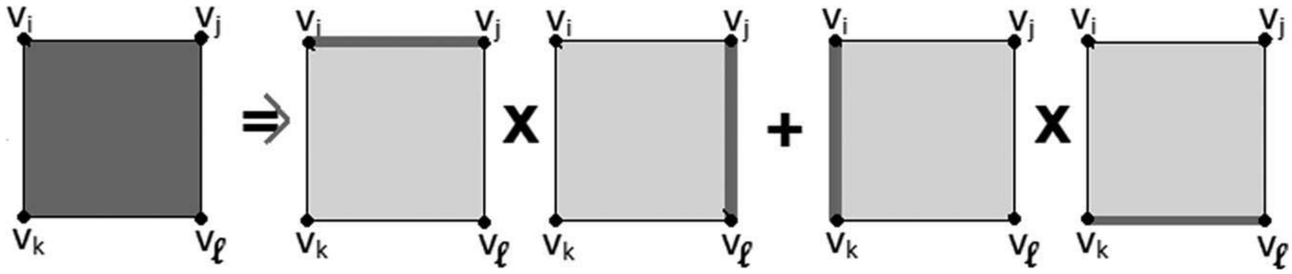

Figure 4. Scheme of the cubical cup product.

$$\phi'\partial'(e)+\partial'\phi'(e)=\phi'\partial(B)+\partial'(\alpha_2+\phi(B)$$
$$+\langle\alpha,\phi(B)\rangle(\alpha+\alpha_1+\alpha_2))$$
$$=\phi\partial(B)+\partial(\alpha_2)+\partial\phi(B)=e+gf(B)=e+g'f'(e).$$
(recall that $f(A)=f(B)=f(e)$ because $f\partial=0$ in an AT $-$ model).

$$\phi'\partial'(\sigma)+\partial'\phi'(\sigma)=\phi'(\partial(\sigma)+\langle\alpha,\partial(\sigma)\rangle\alpha)$$
$$+\langle\alpha,\partial(\sigma)\rangle\phi'(\alpha_1+\alpha_2)$$
$$+\partial'(\phi(\sigma)+\langle\alpha,\phi(\sigma)\rangle\alpha)+\langle\alpha,\phi(\sigma)\rangle\phi'(\alpha_1+\alpha_2)$$
$$=\phi(\partial(\sigma)+\langle\alpha,\partial(\sigma)\rangle\alpha)+\langle\alpha,\phi(\partial(\sigma)$$
$$+\langle\alpha,\partial(\sigma)\rangle\alpha)(\alpha+\alpha_1+\alpha_2)+\langle\alpha,\partial(\sigma)\rangle\phi(\alpha)$$
$$+\partial(\phi(\sigma)+\langle\alpha,\phi(\sigma)\rangle\alpha)+\langle\alpha,\partial(\phi(\sigma)$$
$$+\langle\alpha,\phi(\sigma)\rangle\alpha)\rangle(\alpha+\alpha_1+\alpha_2)+\langle\alpha,\phi(\sigma)\rangle\partial(\alpha)$$
$$=\sigma+gf(\sigma)+(\langle\alpha,\phi\partial(\sigma)\rangle+\langle\alpha,\partial\phi(\sigma)\rangle)(\alpha+\alpha_1+\alpha_2)$$
$$=\sigma+gf(\sigma)+\langle\alpha,\sigma+gf(\sigma)\rangle(\alpha+\alpha_1+\alpha_2)$$
$$=\sigma+g(f(\sigma)+\langle\alpha,f(\sigma)\rangle\alpha)+\langle\alpha,g(f(\sigma)$$
$$+\langle\alpha,f(\sigma)\rangle\alpha)\rangle(\alpha+\alpha_1+\alpha_2)$$
$$+\langle\alpha,f(\sigma)\rangle(g(\alpha)+\alpha+\alpha_1+\alpha_2)$$
$$=\sigma+g'(f(\sigma)+\langle\alpha,f(\sigma)\rangle\alpha)+\langle\alpha,f(\sigma)\rangle g'(\alpha_1)=\sigma+g'f'(\sigma).$$

Observe that $h: C(H)\to C(H')$, given by $h(\alpha)=\alpha_1$ if $\alpha\in H$ and $h(\sigma)=\sigma$ for any $\sigma\in H\backslash\{\alpha\}$, is a chain-group isomorphism. ■

3. 3D CUBICAL COHOMOLOGY RING

In (Niethammer et al., 2002; Kaczynski et al., 2004), the authors consider cubical complexes as the geometric building blocks to compute the homology of digital images. In this section, we adapt, to the cubical setting, the method developed in (Gonzalez-Diaz and Real, 2003, 2005) for computing the simplicial cohomology ring of 3D binary-valued digital photographs. We must mention (Serre, 1951; Kadeishvili and Hopf, 1998) as related works dealing with the cup product on cubical chain complexes in a theoretical context.

Notice that, in 3D, the only non trivial cup products are those corresponding to elements of cohomology of dim. 1. If the cup product of two elements of cohomology of dim. 1 is not zero, then it is a sum of elements of cohomology of dim. 2. Recall that given an AT-model (P, H, f, g, ϕ) for a polyhedral cell complex P, it is satisfied that H is isomorphic to the homology and to the cohomology of P.

A. Cohomology Ring of Simplicial Complexes. We recall now how the cup product is defined in the simplicial setting using AT-models.

Definition 4. (Gonzalez-Diaz and Real, 2003, 2005). Let K be a simplicial complex. It is assumed that the vertices of K are ordered. Let (K, H, f, g, ϕ) be an AT-model for K. Let $\{\beta_1,\dots,\beta_q\}$ be the set of 2-simplices of H and let α_1 and α_2 be two edges of H. The cup product of α_1 and α_2 is:

$$\alpha_1\smile\alpha_2 := \sum_{k=1}^{q}((\alpha_1 f\smile\alpha_2 f)(g(\beta_k)))\beta_k \;\; mod\ 2;$$

where $\alpha_1 f\smile\alpha_2 f$ on a 2-simplex (v_i, v_j, v_k) with vertices $v_i<v_j<v_k$ is $\langle\alpha_1, f(v_i,v_j)\rangle\cdot\langle\alpha_2, f(v_j,v_k)\rangle$; and $(\alpha_1 f\smile\alpha_2 f)$ is extended to 2-chains (sums of 2-simplices) by linearity. Observe that for each k, $g(\beta_k)$ is a sum of 2-simplices representing one cavity. Then, $(\alpha_1 f\smile\alpha_2 f)(g(\beta_k))$ is a sum of 0s and 1s over $Z/2$ whose result is 0 or 1. Therefore, $\sum_{k=1}^{q}((\alpha_1 f\smile\alpha_2 f)(g(\beta_k)))\beta_k$ is a sum of 2-simplices of H of dim. 2, representing the cavities obtained by ''multiplying'' the two representative cycles $g(\alpha_1)$ and $g(\alpha_2)$ (think of the two tunnels of a hollow torus).

It is known that two objects with non isomorphic cohomology rings are not topologically equivalent (more precisely, they are not homotopic) (Munkres, 1984). To use the information of the cohomology ring for this aim, one can construct both matrices M and M' collecting the results of the cup product of cohomology classes of

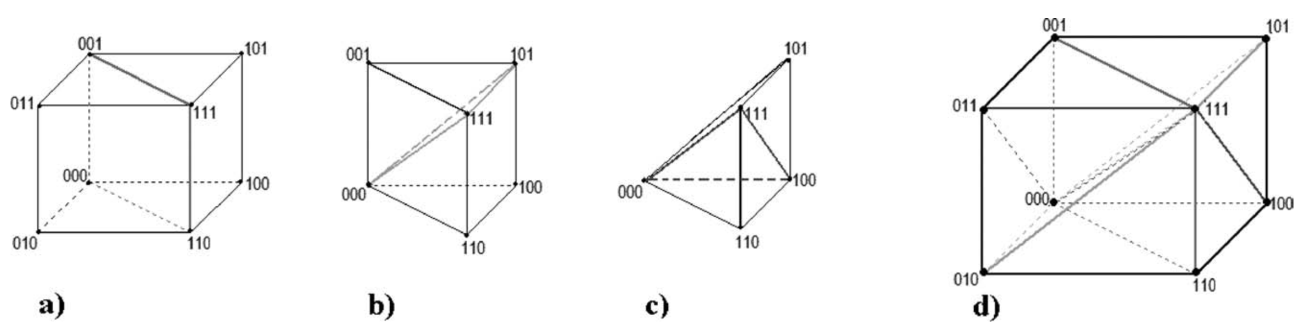

Figure 5. From (a) to (c), successive subdivisions; (d) a cube subdivided in six tetrahedra.

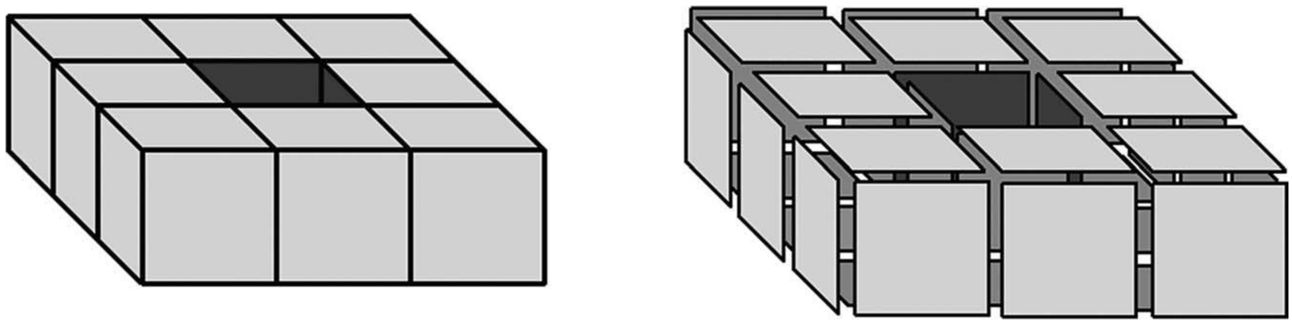

Figure 6. On the left, a 3D binary digital picture $I = (Z^3, 26, 6, B)$. On the right, the set of squares of ∂Q.

dim. 1 of each object. If the rank of M and M' are different, then we can assert that both objects are not homotopic (see (Gonzalez-Diaz and Real, 2005)).

B. Cohomology Ring of Cubical Complexes. In this section, we explain how to obtain a direct formula for the cup product on cubical complexes without making use of any triangulation.

Definition 5. Let Q be a cubical complex. We say that Q satisfies Property P1 if the vertices of Q are labeled in a way that each square (v_i, v_j, v_k, v_ℓ) of Q with vertices $v_i < v_j < v_k < v_\ell$ has the edges (v_i, v_j), (v_i, v_k), (v_j, v_ℓ), and (v_k, v_ℓ) in its boundary.

For example, a cubical complex whose set of vertices is a subset of Z^3 (the set of points with integer coordinates in 3D space R^3) with vertices labeled using the lexicographical order, satisfies P1.

Definition 6. Let Q be a cubical complex satisfying P1 and (Q, H, f, g, ϕ) an AT-model for Q. Let $\{\beta_1, \ldots, \beta_q\}$ be the set of squares of H and let α_1 and α_2 be two edges of H. The cup product of α_1 and α_2 is:

$$\alpha_1 \smile_Q \alpha_2 := \sum_{k=1}^{q}((\alpha_1 f \smile_Q \alpha_2 f)(g(\beta_k)))\beta_k \quad mod\ 2;$$

where $\alpha_1 f \smile_Q \alpha_2 f$ on a square (v_i, v_j, v_k, v_ℓ) with vertices $v_i < v_j < v_k < v_\ell$ (see Fig. 4) is:

$$\langle \alpha_1, f(v_i, v_j)\rangle \cdot \langle \alpha_2, f(v_j, v_\ell)\rangle + \langle \alpha_1, f(v_i, v_k)\rangle \cdot \langle \alpha_2, f(v_k, v_\ell)\rangle;$$

and $(\alpha_1 f \smile_Q \alpha_2 f)$ is extended to 2-chains (sum of squares) by linearity.

Example 2. Let Q be an abstract cubical representation of the hollow torus given in Figure 2. Consider the AT-model (Q, H, f, g, ϕ) for Q, given in Example 1. Recall that $H = \{v_0, (v_0, v_2), (v_0, v_4), (v_0, v_2, v_4, v_8)\}$; $g(v_0) = v_0$, $g(v_0, v_2) = (v_0, v_1) + (v_1, v_2) + (v_0, v_2)$, $g(v_0, v_4) = (v_0, v_3) + (v_3, v_4) + (v_0, v_4)$ and $g(v_0, v_2, v_4, v_8)$ is the sum of the squares of Q, representing the connected component, the two tunnels and the cavity, respectively.

Apply the formula given in Definition 6 in order to obtain the cup product of (v_0, v_2) and (v_0, v_4) in H:

$$\begin{aligned}
&((v_0, v_2)^* f \smile_Q (v_0, v_4)^* f)(g(v_0, v_2, v_4, v_8)) \\
&\quad := \langle (v_0, v_2),\ f(v_0, v_2)\rangle \cdot \langle (v_0, v_4),\ f(v_2, v_8)\rangle \\
&\qquad + \langle (v_0, v_2),\ f(v_0, v_4)\rangle \cdot \langle (v_0, v_4),\ f(v_4, v_8)\rangle \\
&\quad = 1 \cdot 1 + 0 \cdot 0 = 1.
\end{aligned}$$

Then, $(v_0, v_2) \smile_Q (v_0, v_4) = (v_0, v_2, v_4, v_8)$.

The following theorem shows the validity of the definition of $\smile_Q$ (Definition 6). That is, it is stated that we obtain the same result by applying the formula of Definition 6 to compute the cup product on the cubical complex, than making first a triangulation to obtain a simplicial complex, and applying the classical definition of the cup product given in Definition 4, afterward.

Consider successive subdivisions of each cube of a given cubical complex Q until each one is converted in six tetrahedra, and such that each square (v_i, v_j, v_k, v_ℓ) of Q with vertices $v_i < v_j < v_k < v_\ell$ is subdivided by the edge (v_i, v_ℓ) (see Fig. 5d). Let us denote this resulting simplicial complex by K_Q. Observe that with this particular subdivision, if (v_p, v_q, v_r) is a 2-simplex of K_Q, with $v_p < v_q < v_r$, obtained by a subdivision of a square of Q, then (v_p, v_q) and (v_q, v_r) will correspond to edges in Q.

Theorem 1. Let (Q, H, f, g, ϕ) be an AT-model for Q. Let α and α' be two edges of H. Let (K_Q, H', f', g', ϕ') be the AT-model for K_Q

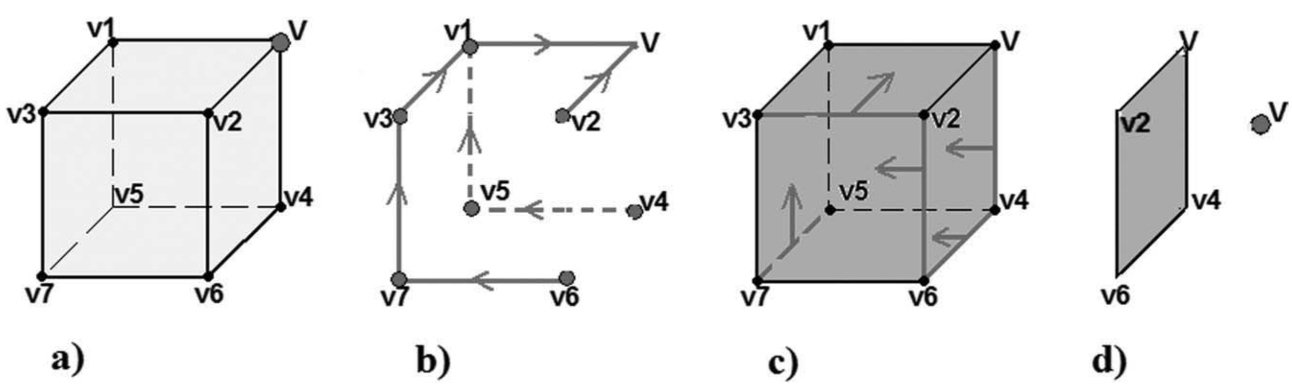

Figure 7. (a) A hollow cube; (b) a spanning tree T with root v; (c) the "path" c_b, for each edge b that does not belong to T; (d) the cells of H.

Table II. An AT-model for the hollow cube given of Figure 7

	∂Q	f	ϕ	H	g
Step 1	v	v	0	v	v
	v_i, $i = 1, \ldots, 7$	v	$\gamma(v_i, v)$		
Step 2	Any edge $b \in Q \backslash T$	0	c_b		
Step 3	(v,v_2,v_4,v_6)	(v,v_2,v_4,v_6)	0	(v,v_2,v_4,v_6)	C

obtained after successively applying Lemma 1. Then,

$$\alpha \smile_Q \alpha' = (\alpha \smile \alpha')h$$

where $\smile$ is the simplicial cup product given in Definition 4, $\smile_Q$ is the cubical cup product given in Definition 6, and $h : C(H) \to C(H')$ is the isomorphism defined at the end of Section 2.

Proof. Observe that since α and α' are edges of H, then $\alpha, \alpha' \in H'$, that is, $h(\alpha) = \alpha$ and $h(\alpha') = \alpha'$. Observe also that $f(a) = f'(a)$ for any edge a because $\beta \notin f(a)$.

We must prove that $(\alpha f \smile_Q \alpha' f)(g(\beta)) = (\alpha f' \smile \alpha' f')(g'(h(\beta)))$. Let $\beta = (v_i, v_j, v_k, v_\ell)$. Let $\beta_1 = (v_i, v_j, v_\ell)$ and $\beta_2 = (v_i, v_k, v_\ell)$ be the two triangles obtained after subdividing β by the edge $e = (v_i, v_\ell)$. Remember that $h(\beta) = \beta_1$ and $g'(h(\beta)) = g'(\beta_1)$. Notice that $g'(\beta_1)$ coincides with $g(\beta)$ if we replace β by $\beta_1 + \beta_2$ in the expression of $g(\beta)$. Therefore, it is enough to prove that $(\alpha f \smile_Q \alpha' f)(\beta) = (\alpha f' \smile \alpha' f')(\beta_1 + \beta_2)$:

$$\begin{aligned}
&(\alpha f \smile_Q \alpha' f)(\beta) = (\alpha f \smile_Q \alpha' f)(v_i, v_j, v_k, v_\ell) \\
&= \langle \alpha, f(v_i, v_j)\rangle \cdot \langle \alpha', f(v_j, v_\ell)\rangle + \langle \alpha, f(v_i, v_k)\rangle \cdot \langle \alpha', f(v_k, v_\ell)\rangle \\
&= \langle \alpha, f'(v_i, v_j)\rangle \cdot \langle \alpha', f'(v_j, v_\ell)\rangle + \langle \alpha, f'(v_i, v_k)\rangle \cdot \langle \alpha', f'(v_k, v_\ell)\rangle \\
&= (\alpha f' \smile \alpha' f')(\beta_1 + \beta_2).
\end{aligned}$$

This concludes the proof. ■

4. CUBICAL COHOMOLOGY RING OF 3D DIGITAL PHOTOGRAPHS

In this section, we develop the main bulk of this article: beginning from a cubical complex Q that represents a 3D binary digital picture whose foreground has one connected component, we first compute an AT-model for the boundary ∂Q of the object; then, having in mind that the homology of ∂Q contains the homology of Q, we obtain an AT-model for Q with the representative cycles of homology generators lying in ∂Q; finally, applying the formula given in Section 3, the cohomology ring is computed from such an AT-model.

A. From Digital Photographs to Cubical Complexes Each point of Z^3 can be identified with a unit cube (called voxel) centered at this point, with facets parallel to the coordinate planes. This gives us an intuitive and simple correspondence between points in Z^3 and voxels in R^3.

Consider a 3D binary digital picture $I = (Z^3, 26, 6, B)$, where B (the foreground) is finite, having Z^3 as the underlying grid and fixing the 26-adjacency for the points of B and the 6-adjacency for the points of $Z^3 \backslash B$ (the background). We say that a voxel V is in the boundary of I if $V \in B$ (i.e., if the point of Z^3 identified with V is in B) and V has a 6-neighbor in $Z^3 \backslash B$.

Take the cubical complex Q for B whose elements are the unit cubes (voxels) centered at the points of B together with all their faces. Observe that this cubical complex, with vertices labeled by the corresponding Cartesian coordinates and considering the lexicographical order, satisfies (P1) (see Definition 5).

Without lack of generality, we consider that the foreground is connected.

The elements of ∂Q are all the squares of Q which are shared by a voxel of B and a voxel of $Z^3 \backslash B$ together with all their faces.

In Figure 6, an example of a 3D digital picture and the squares considered in ∂Q is shown.

B. AT-Model for ∂Q Our interest now is to adapt the incremental algorithm for computing an AT-model given in (Gonzalez-Diaz and Real, 2003, 2005) to the particular complex ∂Q.

First, consider the set of edges and vertices of ∂Q as a graph and compute a spanning forest T. Let $T_1, \ldots, T_m$ be the trees of T corresponding to the connected components of ∂Q. Fixed i, $i = 1, \ldots, m$, take a vertex v_i of T_i and consider it as the root of T_i.

Algorithm 1. *Computing an AT-model* $(\partial Q, H, f, g, \phi)$ *for* ∂Q.
INPUT: The complex ∂Q,
the set $\{T_1, \ldots, T_m\}$ of trees of a spanning forest T of ∂Q,
the set $\{v_1, \ldots, v_m\}$ of roots of the trees of T.

1. Initialize $f(\sigma) := \sigma$, $\phi(\sigma) := 0$ for each $\sigma \in \partial Q$; $H := \{v_1, \ldots, v_m\}$,
   $U := \{v : v \text{ is a vertex of } \partial Q\}$,
   $f(v) := v_i$ *if v is a vertex of* T_i for some i, $i = 1, \ldots, m$.
   For $i = 1$ to m do
   From $\ell = 1$ to the height of T_i do
   For each vertex v at level ℓ, and edge a linking v with its parent w do
   $\phi(v) := a + \phi(w)$, $U := U \cup \{a\}$, $f(a) := 0$.

2. Althrough there are edges in $\partial Q \backslash U$ do
   If there is a square $c \in \partial Q \backslash U$ with exactly one edge $a \in \partial Q \backslash U$ in its boundary:
   $U := U \cup \{c, a\}$,
   $f(a) := f(\partial(c) + a)$, $\phi(a) := c + \phi(\partial(c) + a)$, $f(c) := 0$.

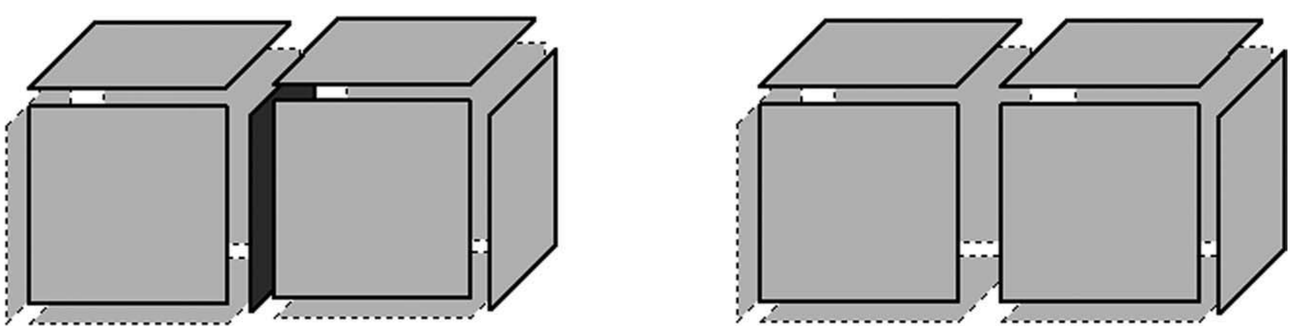

Figure 8. On the left, the squares in the boundary of two cubes c and σ sharing a square σ' (in bold). On the right, the squares of $\partial(c) = \partial(c + \sigma)$.

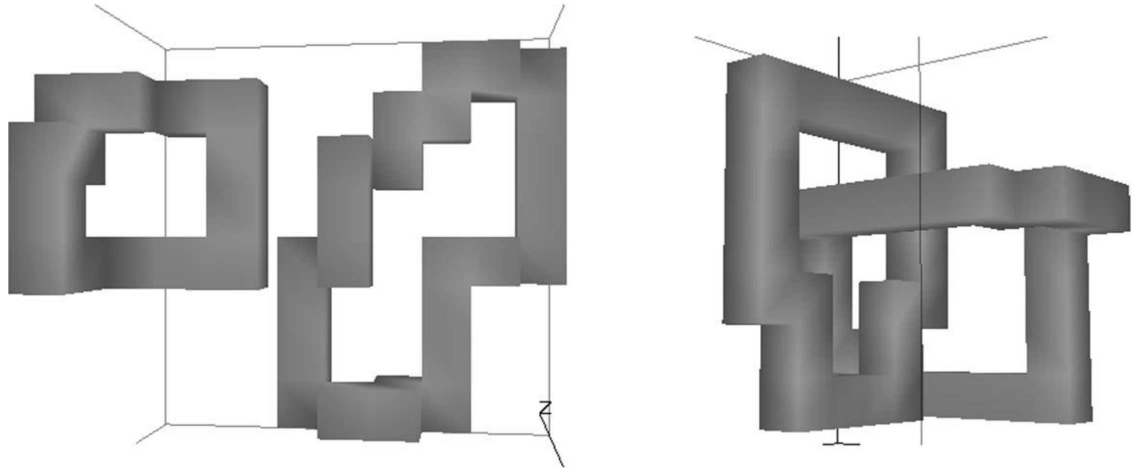

Figure 9. On the left, two non-linked circles. On the right, two once-linked circles.

Else take an edge $a \in \partial Q \backslash U$ then: $H := H \cup \{a\}$, $U := U \cup \{a\}$.
3. Althrough there is a square c in $\partial Q \backslash U$ do $U := U \cup \{c\}$.
If $f\partial(c) = 0$ then $H := H \cup \{c\}$.
Else take an edge a in $f\partial(c)$ then $H := H \backslash \{a\}$.
For each edge b in $\partial Q \backslash T$ do $f(b) := f(b) + \langle a, f(b)\rangle f\partial(c)$,
$\phi(b) := \phi(b) + \langle a, f(b)\rangle (c + \phi\partial(c)), f(c) = 0$.
4. For each $\sigma \in H$ do $g(\sigma) := \sigma + \phi\partial(\sigma)$.
OUTPUT: the AT-model $(\partial Q, H, f, g, \phi)$ for ∂Q.

The auxiliary set U is defined to indicate the cells which have already been used. In Step 1, neither the vertices nor the edges of T_i create cycles except for the root v_i. In Step 3, if a square has edges in its boundary that created cycles in a previous step, then one of these cycles is destroyed. Otherwise, this square creates a new cycle (a cavity). In the last step, the representative cycles of homology generators are computed.

Observe that all the steps of Algorithm 1 are quadratic in the number of elements of ∂Q (worst-case complexity) except for the last part of Step 3 which is cubic in the number of edges of $\partial Q \backslash T$.

Example 3. The AT-model $(\partial Q, H, f, g, \phi)$ of a hollow cube ∂Q (see Fig. 7) is given in the Table II, where $\gamma_{\{(v_i}, v)\}$ is the only path in T from v_i to v; c_b is the square at which the arrow corresponding to an edge b in Figure 7c points, except for $c_{\{(v_4}, v_6)\}$ which is $(v_4, v_5, v_6, v_7) + (v_1, v_3, v_5, v_7)$; and C is the sum of the six squares of ∂Q.

Example 4. The AT-model $(\partial Q, H, f, g, \phi)$ of a hollow cube ∂Q (see Fig. 7) is given in the Table II, where $\gamma_{\{(v_i}, v)\}$ is the only path in T from v_i to v; c_b is the square at which the arrow corresponding to an edge b in Figure 7c points, except for $c_{\{(v_4}, v_6)\}$ which is $(v_4, v_5, v_6, v_7) + (v_1, v_3, v_5, v_7)$; and C is the sum of the six squares of ∂Q.

C. AT-Model for the Cell Complex *K* Topologically Equivalent to *Q*. Now, we use a face reduction technique (see, for example, Kaczynski et al., 2004; Gonzalez-Diaz et al., 2008; Peltier et al., 2009) to obtain a cell complex K which has far fewer cells than Q, such that homology, cohomology and cohomology ring of K coincide with that of Q, and the cells of ∂Q are also cells of K.

Algorithm 2. *Face Reduction Process*.
INPUT: A cubical complex Q.
Initially, $K := Q$.
While there exist $\sigma, \sigma' \in Q \backslash \partial Q$ such that σ' is in $\partial(\sigma)$ do
For each cell $c \in K$ such that σ' is in $\partial(c)$ do
redefine $\partial(c)$ as $\partial(c + \sigma)$.
Remove σ and σ' from the current K;
OUTPUT: the cell complex K.

See Figure 8 as an example of face reduction.

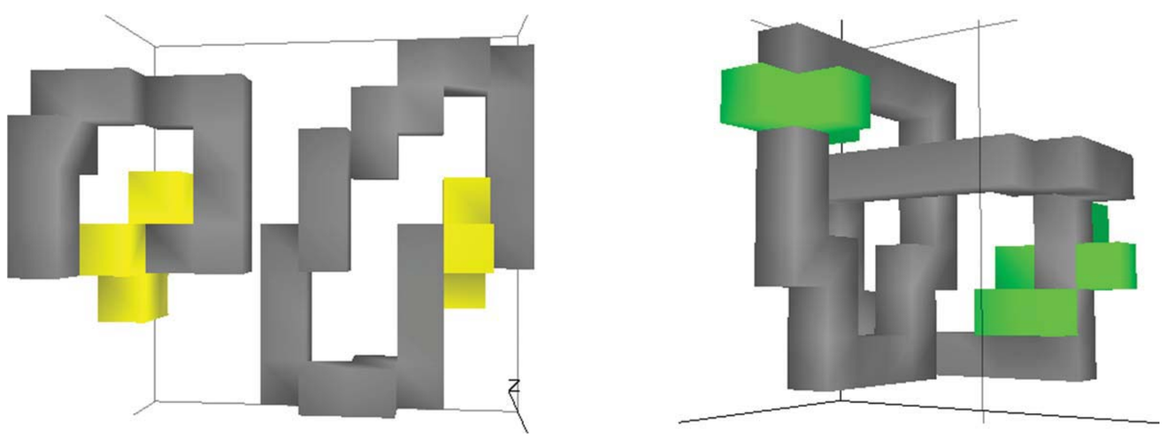

Figure 10. On the left, representative cycles of the two tunnels of Q_1'. On the right, representative cycles of the two tunnels of Q_2'. [Color figure can be viewed in the online issue, which is available at wileyonlinelibrary.com.]

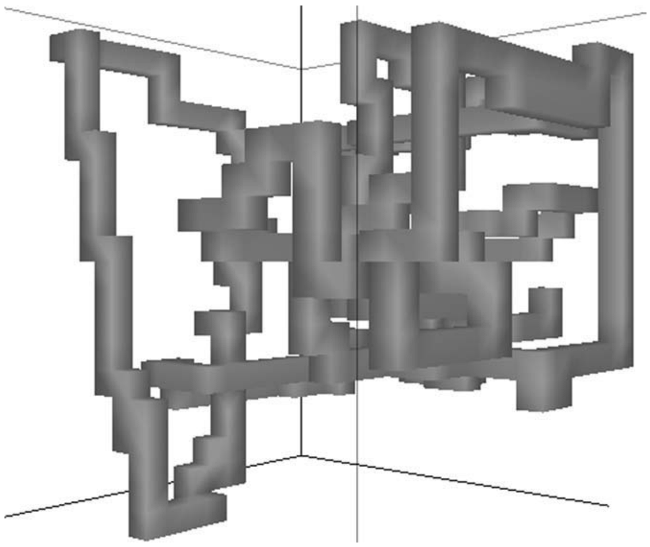

Figure 11. A configuration of seven linked circles (picture of size 20×20×20)

Observe that after the face reduction process, we obtain a cell complex K with the same topological information as Q but with fewer cells. Now, starting from an AT- model for ∂Q, compute an AT-model for K adding the cells of $K \backslash \partial Q$ incrementally as follows:

Algorithm 3. *AT-model for K*.

INPUT: An AT-model for ∂Q: $(\partial Q, H, f, g, \phi)$ and the cells $\{\sigma_1, \ldots, \sigma_m\}$ of $K \backslash \partial Q$ ordered by increasing dimension.

Initially, $f_K(\sigma) := f(\sigma)$, $\phi_K(\sigma) := \phi(\sigma)$, $g_K(\sigma) = g(\sigma)$ for each $\sigma \in \partial Q$;

$f_K(\sigma) := 0$, $\phi_K(\sigma) := 0$, for each $\sigma \in K \backslash \partial Q$; $H_K := H$.

For $i = 1$ to $i = m$ do:

Take a cell, σ, of $f_K \partial(\sigma_i)$, then $H_K := H \setminus \{\sigma\}$,

For $k = 1$ to $k = i - 1$ do

$f_K(\sigma_k) := f_K(\sigma_k) + \langle \sigma, f_K(\sigma_k) \rangle f_K \partial(\sigma_i)$

$\phi_K(\sigma_k) := \phi_K(\sigma_k) + \langle \sigma, f_K(\sigma_k) \rangle (\sigma_i + \phi_K \partial(\sigma_i))$

OUTPUT: the AT-model $(K, H_K, f_K, g_K, \phi_K)$ for K.

Observe that, in the algorithm, a cycle is never created because the set of the homology generators of K is a subset of the homology generators of ∂Q. Therefore, when a cell σ_i of K is added, then $f_K \partial(\sigma_i)$ is never null and then a class of homology is always eliminated (that is, a cell σ of f_K \partial (σ_i) is removed from H_K).

The worst-case complexity of Algorithm 3 is $O(m^3)$, where m is the number of cells of $K \backslash \partial Q$. Observe that m is also the number of generators of the homology of ∂Q minus the number of generators of Q.

Table III. The multiplication tables for the cup product on Q_1' and Q_2'

Q_1'	$\alpha_1 \smile_Q \alpha_1$	$\alpha_1 \smile_Q \alpha_2$	$\alpha_2 \smile_Q \alpha_2$
β_1	0	0	0
β_2	0	0	0
Q_1'	$\alpha_1' \smile_Q \alpha_1'$	$\alpha_1' \smile_Q \alpha_2'$	$\alpha_2' \smile_Q \alpha_2'$
β_1'	0	1	0
β_2'	0	1	0

The cubical complexes associated with the background of the photographs given in Figure 10, where α_i (resp. α_i'), $i = 1,2$, are representative cycles of the two tunnels of Q_1' (resp. Q_2'); and β_i (resp. β_i'), $i = 1,2$, are representative cycles of the two cavities of Q_1 (resp. Q_2).

Table IV. The multiplication table for the cup product of the cubical complex associated to the white voxels of the photograph in Figure 12, where ''CP *i j*'' denotes the sum of the cavities *i* and *j*

	α_1	α_2	α_3	α_4	α_5	α_6	α_7
α_1		–	–	–	–	–	–
α_2			–	–	–	–	–
α_3				-	CP 3 5	CP 3 6	–
α_4					CP 4 5	–	–
α_5						-	CP 5 7
α_6							CP 6 7
α_7							

D. Cohomology Ring of the Cell Complex *K* Topologically Equivalent to *Q* Given a digital picture $(Z^3, 26, 6, B)$, the cubical complex Q associated with it, and having computed an AT-model $(K, H_K, f_K, g_K, \phi_K)$ for K, the last step of the process is the computation of the cohomology ring. This can be performed using the formula for the cubical cup product given in Definition 5.

Example 5. This example shows an application of $\smile_Q$ to discriminate different embeddings of the same object. Consider the cubical complex Q_1 (resp. Q_2) associated with a digital picture where the set B consists in two once-linked ''circle'' (resp. two unlinked ''circles''). See Figure 9. Both complexes have two tunnels and no cavities, so these properties are not able to distinguish them. Now, denote by Q_1' and Q_2', the cubical complexes associated with the background of I_1 and I_2 (white voxels of Fig. 9). Compute an AT-model for Q_1' and its cohomology ring, for $i = 1,2$. We obtain that the multiplication table for the cup product on Q_1' is null whereas on Q_2' is not (see Fig. 10 and Table III). This fact allows us to assert that the background of I_1 and I_2 are not topologically equivalent. This problem has been pointed out in (Kropatsch, 2002).

Example 6. Consider the picture in Figure 11. The cubical complex associated with the white voxels of the picture has 1 connected component, 7 tunnels, and 12 cavities. The results of the computation of the cup product can be seen in Table IV).

Now, let Q be a cubical complex with m cells. Let q be the number of cavities of Q, let m_1 (resp. m_2) be the number of edges (resp. squares) of Q. Observe that, on one hand, we can compute an AT-model for Q in $O(m^3)$ and the cup product of two cohomology classes of Q in $O(m_1^2\, m_2 q)$. On the other hand, using the results of this section, we can compute an AT-model for K in $O(n_1^3 + n^3)$ where n_1 is the number of edges of $\partial Q \backslash T$ and n is the number of homology generators of ∂Q minus the number of homology generators of Q. The cup product of two cohomology classes can be performed in $O(n_1^2\, n_2 q)$ where n_2 is the number of squares of ∂Q. See Table V relating m_1, m_2, m with n_1, n_2, n.

Example 7. Consider the two magnetic resonance images given in Figure 12. The picture on the left, called I_1, consists of 14 slices of size 320 × 320 and the picture on the right, called I_2, consists of 25

Table V. Number of vertices, edges, squares and cubes of the cubical complexes Q_i and ∂Q_i, associated with the photographs I_i, $i = 1,2$, of Figure 13

	Q_1	∂Q_1	Q_2	∂Q_2
Number of vertices	183,593	85,084	646,332	298,075
Number of edges	500,252	170,321	1,778,591	602,360
Number of squares	453,733	85,532	1,622,249	304,738
Number of cubes	136,989	0	489,960	0

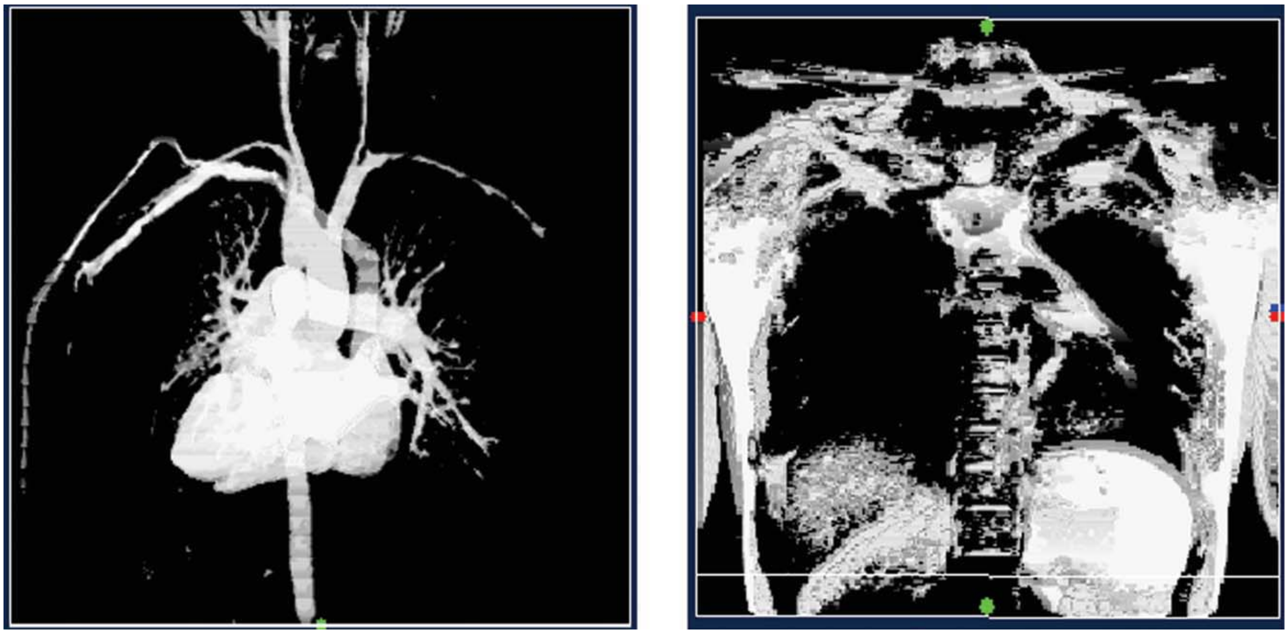

Figure 12. On the left, a magnetic resonance angiography of the heart (picture I_1 of size 320×320×14) and, on the right, a magnetic resonance image of the torax (picture I_2 of size 240×240×25), after a binarization process. [Color figure can be viewed in the online issue, which is available at wileyonlinelibrary.com.].

slices of size 340 × 240. In Table V, the number of the vertices, edges, squares and cubes of Q_i and ∂Q_i, the cubical complexes associated with I_i, $i = 1,2$, is given. Our naïve implementation of the algorithms only permits photographs of maximum size 100×100×100. After subsampling the two photographs we obtain another two, called I_1' and I_2', of size 80 × 80 × 14 and 84 × 84 × 25 (see Fig. 13). In Table VI, the number of cells of Q_i' and K_i', the cubical complexes associated with I_i', $i = 1,2$, and the number of connected components, tunnels and cavities of both I_2^1 and I_1^1 are given.

E. From Cubical Complexes to Digital Photographs Now, given a digital photograph I, suppose that we have computed an AT-model (K, H_K, f_K, g_K, ϕ_K) for K, following the steps given in Subsections A–C. For each σ in H_K, $g_K(\sigma)$ is a representative cycle of a homology generator of K and, therefore, of Q, since the homology of K and Q coincide and the representative cycles are in ∂Q. Recall that if σ is a vertex, then $g_K(\sigma)$ is a vertex representing a connected component; if σ is an edge, then $g_K(\sigma)$ is a sum of edges representing a tunnel; and if σ is a square, then $g_K(\sigma)$ is a sum of squares representing a cavity.

Given a representative cycle $g_K(\sigma)$ of a homology generator, our aim in this subsection is to draw the equivalent cycle in the picture I.

1 If $g_K(\sigma)$ is a vertex then, $g_K(\sigma)$ is a face of a square in ∂Q. This square is shared by a voxel V of B and a voxel of Z^3/B. Then, associate the voxel V with the vertex $g_K(\sigma)$.
2 If $g_K(\sigma)$ is a sum of edges, suppose that $g_K(\sigma)$ is a simple cycle (if not, it always can be decomposed in simple ones). Visit all the edges of the cycle in order. If an edge, a, and the next edge, b, are facets of a square $\sigma \in \partial Q$, then associate the single voxel V of B which has σ in its boundary, with the edges a and b.

Visit all the edges that have not been associated with any voxel. If a voxel V is associated with the next edge of the current one, a, and there is a voxel $V' \in B$ having a in its boundary, such that V' is in the boundary of I and V' and V are 6-neighbor, then associate V' with a. If not, look at the previous edge and do the same procedure. If not, take any voxel of B that contains a, having a 6-neighbor voxel in $Z^3 \setminus B$.
3 Finally, if $g_K(\sigma)$ is a sum of squares, associate the single voxel V of B which has σ in its boundary, , with each square σ.

See Figure 13 as an example of the procedure.

5. CONCLUSIONS AND FUTURE WORK

In this article, we present formulas to directly compute the cohomology ring of 3D cubical complexes and develop a method for the computation on 3D binary-valued photographs. This computation on cubical complexes can be regarded as a starting point to compute the cup product on general polyhedral cell complexes, which is, in fact, our ultimate goal. The restriction to the 3D-world allows to work over Z/2, what facilitates the calculus. However, a harder task could be to extend the formulas of the cohomology ring to higher dimensions what could be applied to more general contexts out of digital images. In this sense, our starting point could be first, the tools described in (Gonzalez-Diaz et al., 2009d) which are useful to determine homological information in the integer domain of nD structured objects such as simplicial, cubical or simploidal complexes and second, the work on cohomology ring of nD simplicial complexes using AT-models in the integer domain (also called AM-models) developed in (Gonzalez-Diaz et al., 2009c). Another

Table VI. Number of cells of the cell complexes $Q_1'$and K_1' associated with the photographs I_1', $i = 1,2$, of Figure 14 and the number of connected components, tunnels, and cavities of I_1' and I_2'

	Q_1'	K_1'	Q_2'	K_2'
Number of cells	93,441	39,051	739,515	253,181
Number of connected components	59	59	129	129
Number of tunnels	19	19	477	477
Number of cavities	2	2	10	10
Execution time	52 sec	9 sec	Out of memory	30 sec

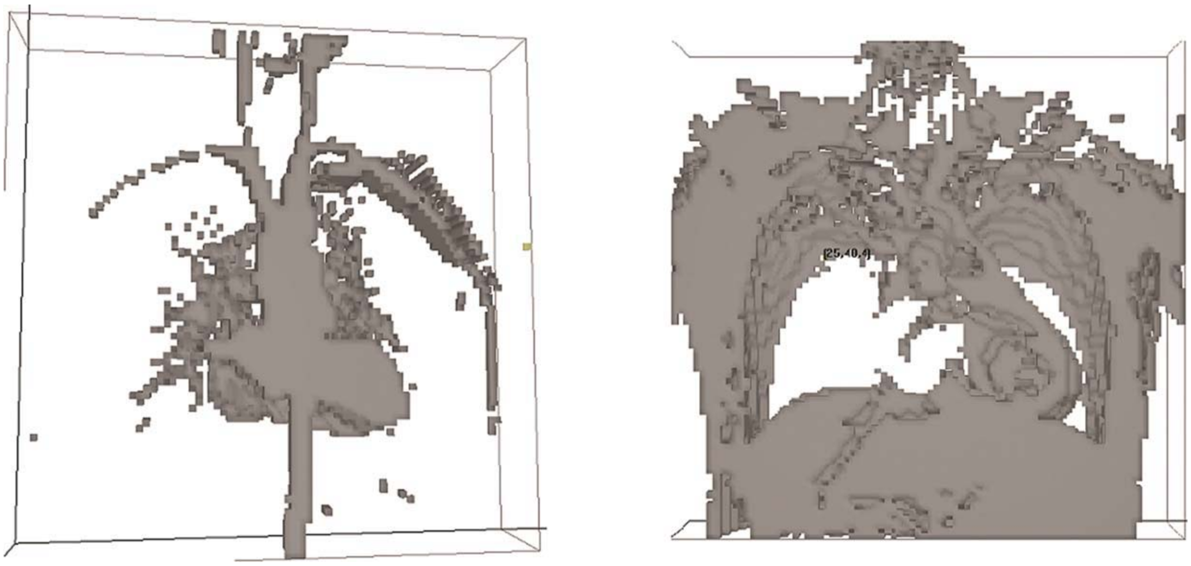

Figure 13. Photographs I_1' (on the left) and I_2' (on the right) after resizing the photographs of Figure 13. [Color figure can be viewed in the online issue, which is available at wileyonlinelibrary.com.]

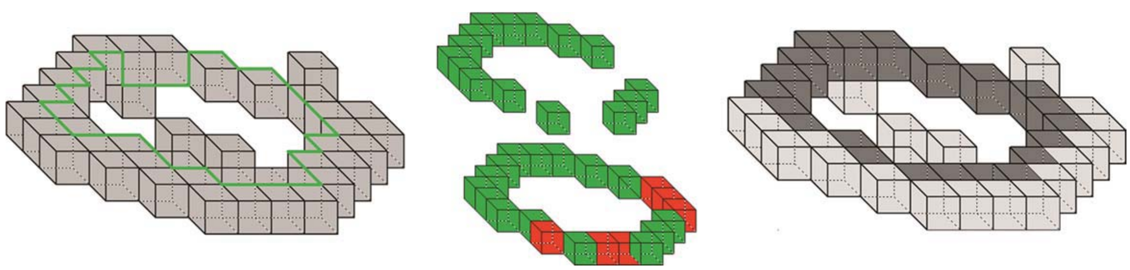

Figure 14. On the left, a representative cycle of a homology generator (the set of edges in bold); On the topcenter, voxels considered the first time the edges of the cycle are visited. On the bottom-center, voxels considered the second time the edges of the cycle are visited. On the right, voxels in bold representing the cycle. [Color figure can be viewed in the online issue, which is available at wileyonlinelibrary.com.]

goal for future work is to adapt our results to irregular graph pyramids and compute the cohomology ring on the cell complexes associated with such structures. In this article (Gonzalez-Diaz et al., 2009a), representative cocycles for cohomology generators on irregular graph pyramids are computed, what can be considered as a first step in this direction.

REFERENCES

P. Alexandroff and H. Hopf, Topologie I, Springer, Berlin,1935.

R. Gonzalez-Diaz, A. Ion, M. Iglesias-Ham, and W.G. Kropatsch, Irregular graph pyramids and representative cocycles of cohomology generators, LNCS 5534 (2009a), 263–272.

R. Gonzalez-Diaz, M.J. Jimenez, and B. Medrano, ''Cohomology ring of 3D cubical complexes,'' In Progress in combinatorial image analysis, P. Wiederhold and R.P. Barneva (Editors), Research Publishing, Singapore 2009b, pp. 139–150.

R. Gonzalez-Diaz, M.J. Jimenez, B. Medrano, H. Molina-Abril, and P. Real, Integral operators for computing homology generators at any dimension, LNCS 5197 (2008), 356–363.

R. Gonzalez-Diaz, M.J. Jimenez, B. Medrano, and P. Real, A tool for integer homology computation: λ-AT-model, Image Vis Comput 27 (2009d) 837–845.

R. Gonzalez-Diaz, M.J. Jimenez, B. Medrano, and P. Real, Chain homotopies for object topological representations, Discrete Appl Math 157 (2009c), 490–499.

R. Gonzalez Diaz and P. Real, On the cohomology of 3D digital images, Discrete App Math 147 (2005), 245–263.

R. Gonzalez-Diaz and P. Real, Towards digital cohomology, LNCS 2886 (2003), 92–101.

T. Kaczynski, K. Mischaikow, and M. Mrozek, Computational homology, Appl Math Sci 157 (2004).

T. Kadeishvili, DG Hopf algebras with steenrods *i*-th coproducts, Bull Georgian Acad Sci 158 (1998), 203–206.

W.G. Kropatsch, Abstraction pyramids on discrete representations, LNCS 2301 (2002), 1–21.

H. Molina-Abril and P. Real, Advanced homological information of digital volume via cell complexes, LNCS 5342 (2008), 361–371.

J. R. Munkres, Elements of algebraic topology, Addison-Wesley Co., Menlo Park, California, 1984.

M. Niethammer, A.N. Stein, W.D. Kalies, P. Pilarczyk, K. Mischaikow, and A. Tannenbaum, Analysis of blood vessel topology by cubical homology, Proc IEEE ICIP 2 (2002), 969–972.

S. Peltier, A. Ion, W.G. Kropatsch, G. Damiand, and Y. Haxhimusa, Directly computing the generators of image homology using graph pyramids, Image Vis Comput 27 (2009), 846–853.

J.P. Serre, Homologie Singuliere des espaces fibres, applications, Ann Math 54 (1951), 429–501.